Research Article GU J Sci, Part A, 10(2): 184-195 (2023) 10.54287/gujsa.1264848

Gazi University
Journal of Science
PART A: ENGINEERING AND INNOVATION
http://dergipark.org.tr/gujsa

Evaluation of Range Estimation Performance of FLIR with Field Requirements Criteria

Buket AKIN[1*]

[1]*Gazi University, Faculty of Science, Department of Physics, Ankara, Türkiye*

Keywords

Forward-Looking Infrared

Thermal Imaging

Infrared System Performance

Abstract

Thermal imaging performance depends on many variables, ranging from the properties of the imaged object to atmospheric transmittance and system parameters. After clarification of the functional needs in system design or procurement, system parameters of the design that can meet these needs should be determined. Diagnosis/recognition from a distance is one of the foremost of these needs. The following briefly introduces the Forward Looking Infrared (FLIR) systems, followed by explanations for calculating the theoretical diagnostic range. After the theoretical information, sample systems are given, and high-performance FLIR systems are presented. To accurately analyze, measure and predict the performance of FLIR systems, a model should calculate summary performance measures of the system in the form of Minimum Resolvable Temperature (MRT) and Modulation Transfer Function (MTF) between a target and its background and estimate range for a given scenario electro-optical required for the performance evaluation of the system. The accuracy of these calculations will ultimately determine the accuracy of the model by which the performance of the FLIR system is evaluated.

Cite

Akın, B. (2023). Evaluation of Range Estimation Performance of FLIR with Field Requirements Criteria. *GU J Sci, Part A, 10*(2), 184-195. doi:10.54287/gujsa.1264848

Author ID (ORCID Number)

0000-0002-9748-4886 Buket AKIN

Article Process

Submission Date 14.03.2023
Revision Date 27.03.2023
Accepted Date 18.04.2023
Published Date 21.06.2023

1. INTRODUCTION

Long-range electro-optical surveillance systems (Javidi, 2006) have been widely used in industrial applications. FLIR, one of these applications, was used for mapping purposes by the US Air Force in the 1960s in the infrared systems looking toward the earth from aircraft. When these systems were modified to develop new systems for imaging purposes, the Forward Looking Infrared (FLIR) was used to distinguish it from downward-facing systems. FLIR can be perceived as a camera that displays in the infrared band. The primary purpose is to perform the function of seeing in the dark by perceiving and processing the natural dispersion created by the objects, and Planck's law explains this spread.

Thermal imagers are intended to utilize the atmospheric transmission window to gather target radiation in the infrared region of the spectrum. Due to variations in IR signature and atmospheric transmission in the scene, the range is impacted by the choice of spectral sensitivity band. The atmosphere is not equally permeable at all wavelengths. The ranges with high permeability are between 3-5μm and 8-14μm. The 3-5μm band is called medium wavelength infrared (MWIR), and the 8-14μm band is called long wavelength infrared (LWIR). The transmittance in these ranges also makes FLIR systems different from other night vision systems. Other night vision systems provide images by amplifying visible light in the environment that is so dimm that human eye cannot perceive. FLIR systems, on the other hand, can provide images in complete darkness, even from behind a curtain of fog and smoke. Every user is interested in knowing the range of these imagers, which is a crucial parameter. The range parameters for these systems can be determined by computer simulations, field testing,

*Corresponding Author, e-mail: bktakn90@gmail.com

or laboratory measurements. Calculating range parameters in computer simulations requires the a priori knowledge of the exact characteristics of the optical system, detector array, signal processing, and imaging modules of a particular thermal imager.

Thermal cameras' detection, recognition, and identification ranges can be determined using many methods. The oldest and most famous of these methods is the Johnson criterion, published in 1958 (Johnson, 1958). It allows an observing device's detection, recognition, and identification ranges (assuming a 50% target discrimination probability) to be determined based on the measured spatial resolution characteristics. Its calculation method is based on how many pixels are adequate to detect, recognize and identify (DRI) an object with 50% probability. For instance, the number of pixels to resolve a human are 3.5x1, 11x3 and 23x6 for DRI, respectively. The minimum resolvable temperature difference (MRTD) or minimum resolvable temperature (MRT) characteristics must be measured to determine thermal camera's detection, diagnosis, and recognition ranges. MRT links Johnson's concept of target critical size resolvable rods and thermal imaging system performance. MRT is the fundamental measurement parameter for evaluating the overall imaging performance of FLIR systems. The value of MRT measurement is determined by incorporating sensitivity (temporal and spatial), resolution, system performance and observer effects. The MRT measurement creates an association between the performance of the thermal imager and the thermal imaging model to deliver the anticipated range value with good precision and reproducibility in real-world settings.

MRT is often the primary imaging requirement specified for a FLIR system, as it is the basis for range estimates. The NATO standards (NATO Standardization Agency, 1995) define the MRT measurement process and the determination of range parameters, and the parameter N50 specifies the number of pairs per target size. Although Johnson's criteria contribute to predicting the range parameters of thermal cameras, they do not provide reliable results in today's systems. The Johnson criteria do not consider image noise levels, electronic circuits used for high-frequency amplification, digital filtering, or interpolation, which impact range performance in such systems. Therefore, the latest, complete and reliable Targeting Mission Performance Metric (TTP) model has been developed by the US Army Night Vision and Electronic Sensors Directorate since 2000 (Schmieder & Weathersby, 1983; Driggers et al., 2000; Vollmerhausen & Driggers, 2000; NATO Research and Technology Organisation, 2003; Moyer et al., 2004; 2006; Vollmerhausen & Jacobs, 2004; Krapels et al., 2006; 2008; Teaney et al., 2007; Vollmerhausen et al., 2010) and the NVThermIP software (U.S. Army Night Vision and Electronic Sensors Directorate, 2001) is based on this model. Based on the 2.7*N50, it was defined as V50 (Krapels et al., 2008). The TTP model is highly sophisticated since it takes the detector, platform, environment, and target specified in the image into account. (Vollmerhausen & Jacobs, 2004; Hou et al., 2022).

Most range estimation models deal with parameter definitions of the imaging system, depending on the scenario, and the range of the image. These models make thermal image analysis and synthesis convenient, which are used to define the best system design. To verify the utility of these models, the results are expanded to range estimation of the images using various techniques, such as visual information detection modeling, target IR signature, and atmospheric route-dependent image distortion (Figure 1). Currently, efforts to use automatic objective target resolution criteria are ongoing. However, current applications have not yet reached the required level of accuracy as it involves developing complex image-processing techniques (Perić et al., 2019; Sagan et al., 2019).

The estimation models of range parameters of thermal imagers are based on the modulation transfer function (MTF). MTF is a fundamental parameter that determines the imaging resolution of the sensor and is utilized in system design and analysis. The diffraction-limited optical system MTF function can be reasonably calculated in terms of the limits defining the resolution of the system and the highest attainable spatial frequency because the MTF function has a known square detector shape (Perić & Livada, 2019; Vollmer, 2021). This parameter is often shown down to the cutoff frequencies and is accurate for all spatial frequencies. The detector array's spatial Nyquist frequency (ξny) must be considered to avoid aliasing effects. Although the detector MTF is the electro-optical system's limiting component, it is typically the mixture of optical and electronic responses that provides the total system MTF because $\xi Ny << \xi cutoff$ in general. The MTF function of a thermal imaging system may be tested in a lab setting, and the MTF function of each subsystem can be

modeled. The system MTF is appropriate for evaluating the effectiveness of system design. In addition, MTF analysis can help identify the root cause of deficiencies in case a system is not performing as expected.

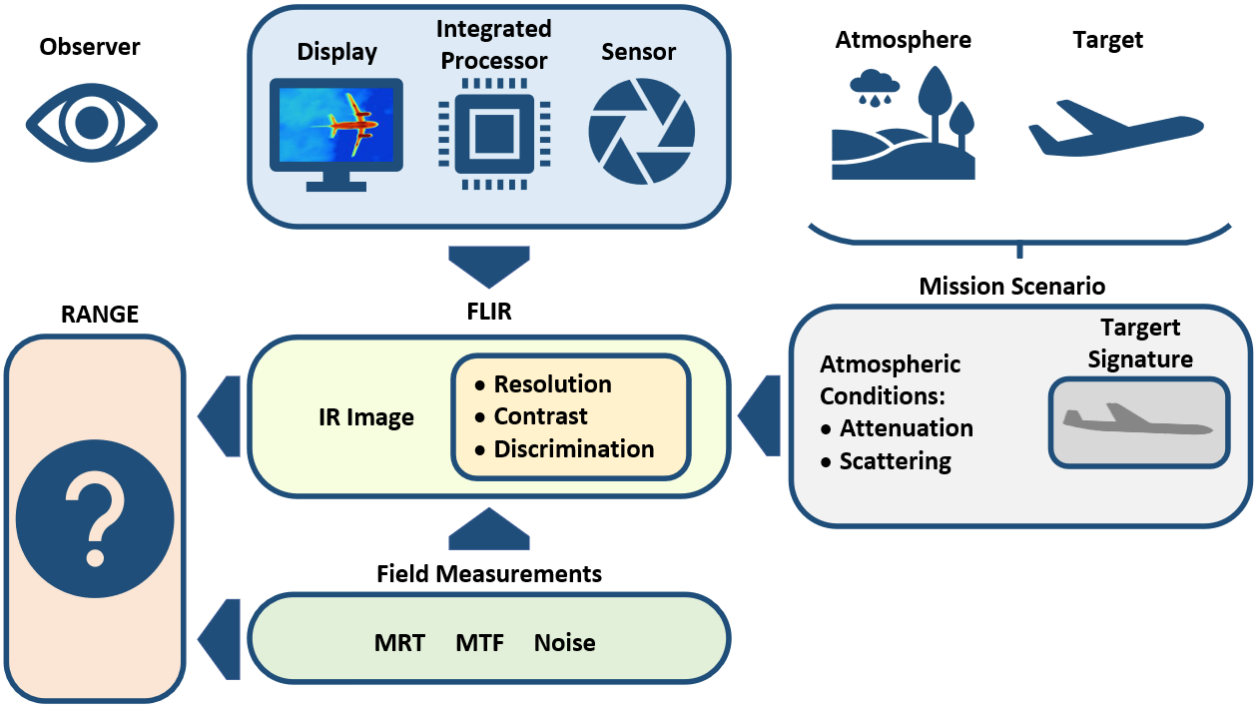

Figure 1. *FLIR Range Estimation Data Sources and Targeting*

To be able to detect and track with the system designed, traditionally, images of a target from different angles are collected, using other cameras with the same wavelength as the system in such a way that the maximum number of pixels falls on the target but, there are specific difficulties in determining thermal imager performance in two stages, moving target detection and target recognition. The first phase involves detecting moving targets in the entire frame using background subtraction from clutter. Background subtraction might not always be possible due to detecting isolated pixels. Therefore, connected components smaller than the object size should be eliminated by clutter rejection.

The second step is processing the image using morphological transformations and fusion to extract the region of interest containing the detected target in the thermal image. The target recognition phase consists of feature extraction and target classification. A CNN-based (convolutional neural network) deep neural network model can be used for target classification. Target classification is training a classifier with extracted features to create a classification model to classify new data. But unlike visual datasets, thermal datasets are limited, and CNNs often do not fare well with test data. To overcome this challenge, the researchers propose using transfer learning, in which deep networks trained on large datasets for a different application or detection method are adapted for another task or data.

This study is to determine the basic electro-optical parameters related to IR thermal imager range estimations and to define how these parameters can be used for range estimation by describing them under field conditions. It is crucial to determine the system parameters correctly before starting the design and to limit the design for cost and time. To make the design fit for the purpose, the fundamental optical parameters such as optical aperture, F/#, focal length, Noise equivalent temperature (NET), and Field of view (FOV) are determined. Performance analyses are performed using MATLAB according to the specified parameters. These parameters may vary according to system requirements. This article presents the range performance analysis of FLIR, which is more compact, lighter, serves more missions, and can identify a target at a distance of 2.4 km.

2. FUNDAMENTALS OF THERMAL IMAGING METHOD

All objects with a temperature above "absolute zero" emit electromagnetic radiation. Calculating this emission with the following formula (1), depending on the temperature and wavelength, is possible.

$$M_e(\lambda,T)=\left(\frac{2\pi hc^2}{\lambda^5}\right)\left[exp\left(\frac{hc}{\lambda kT}\right)-1\right]^{-1}\ [Wm^{-3}] \quad (1)$$

where c is the speed of light in vacuum=2.997x10^{8}ms^{-1}, h is Planck constant=6.626x10^{-34}J.s, k is Boltzman constant=1.381x10^{-23}J.K^{-1}, T is the absolute temperature in Kelvin, and λ refers to wavelength in meter.

The formula (1) is "Planck's black body radiation law". When it is desired to calculate the actual emission from an object, it is used together with the emission value, which depends on the wavelength of the object (Wolfe & Zissis, 1985).

$$[M_e(\lambda,T)]_{real}=E(\lambda,T)M_e(\lambda,T) \quad (2)$$

Since it is the amount of energy per photon (E=hc/λ), Planck's law can be written regarding photon flux as follows:

$$M_q(\lambda,T)=\frac{\lambda}{hc}M_e(\lambda,T)\quad [photon.s^{-1}.m^{-3}] \quad (3)$$

The total energy emitted from an object is obtained by integrating equation (1) at all wavelengths.

$$M_e(T)=\sigma T^4\quad [W.m^{-2}] \quad (4)$$

where σ is Stefan-Boltzmann constant=5.67x10^{-8}W.m^{-2}.K^{-4}.

According to (4), a total power of 460W is emitted from an object with a temperature of 300 K and a surface area of 1m^2.

The variation of the radiated energy concerning the temperature is obtained by taking the derivative of (4) concerning the temperature.

$$\frac{\partial M_e}{\partial T}=4\sigma T^3\quad [W.m^{-2}K^{-1}] \quad (5)$$

Therefore, a 1-degree change in the temperature of a 1 m^2 object at 300 K leads to a change of approximately 6 Watts compared to (5); however, this is the sum across all wavelengths. The 8-14μm range carries about a third of the total energy, accounting for an energy difference of approximately 2 Watts. In summary, if an object with a temperature of 300 Kelvin is observed in the 8-14μm band, the parts with a temperature difference of 1 degree between them will radiate with a total energy difference of about 2 Watts. The detector can detect a significant, tiny portion of this energy difference. This perceived difference will create a visual contrast depending on the temperature difference, and an image will be made this way.

2.1. FLIR Types

FLIR systems are divided into "staring" and "scanning" (scanning). Staring-type FLIR systems use detectors in the form of a focal plane array. On the other hand, scanning systems can be evaluated in two groups "series" and "parallel."

In parallel scanning, each detector in the FLIR scans a line of the image to be acquired. Since the detectors are arrayed one after the other, the whole image is obtained when a "forward scan" is performed as a whole scan

Figure 2. Since the lines between the detectors will not be scanned due to the physical gaps between the detectors, the detectors are shifted by the length of the detector while returning from the end of the line, and a "back-scan" is performed. Thus, there is no unscanned area in the area. When scanning is performed at a frequency so high that the human eye cannot detect (e.g.,> 20 Hz), the resulting image will apperar as a still image.

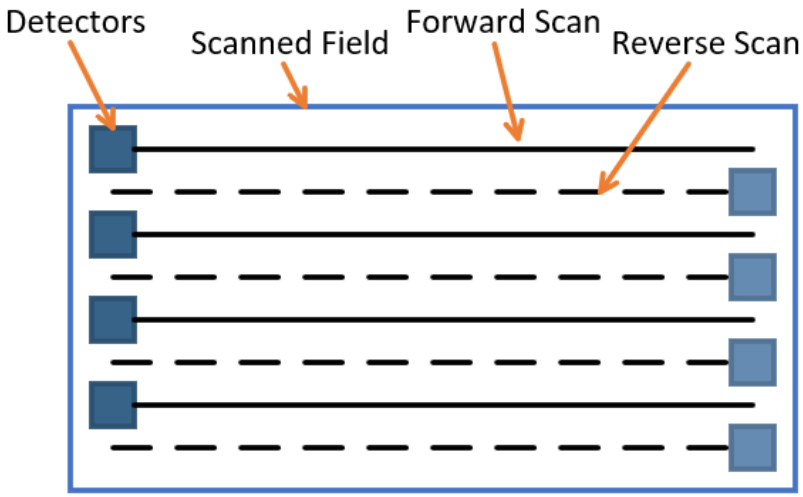

Figure 2. *Detector Scanning Model*

In a serial scan, the detectors in the FLIR are stacked in a row, so they scan the entire image, not just a line, as in parallel scanning. Since the detectors are in a row, the image of the position of the 1st detector at time t will be obtained again when the second detector comes to that position at time t+1. The images obtained by all these cascading detectors are integrated with a process called "time delay integration TDI" Figure 3.

Fixed surveillance, on the other hand, is a type of design that can be realized by integrating many detectors into a series. This design is called Focal Plane Array (FPA). In this design, scanning is unnecessary as the arrays cover entirely the image area.

The main detector types used in FLIR devices are Platinum Silicide (PtSi), Mercury Cadmium Telluride (HgCdTe), Indium Antimonide (InSb), and Gallium Arsenide (GaAs). PtSi Shottky-barrier detectors are the most suitable material for large arrays of 3-5 μm, as they provide high resolution when used as a surveillance array. The cost of these detectors is also low, as their production is based on already advanced silicon technology. Although the quantum efficiency is low due to the large number of detectors in the array, the sensitivity of the device is high.

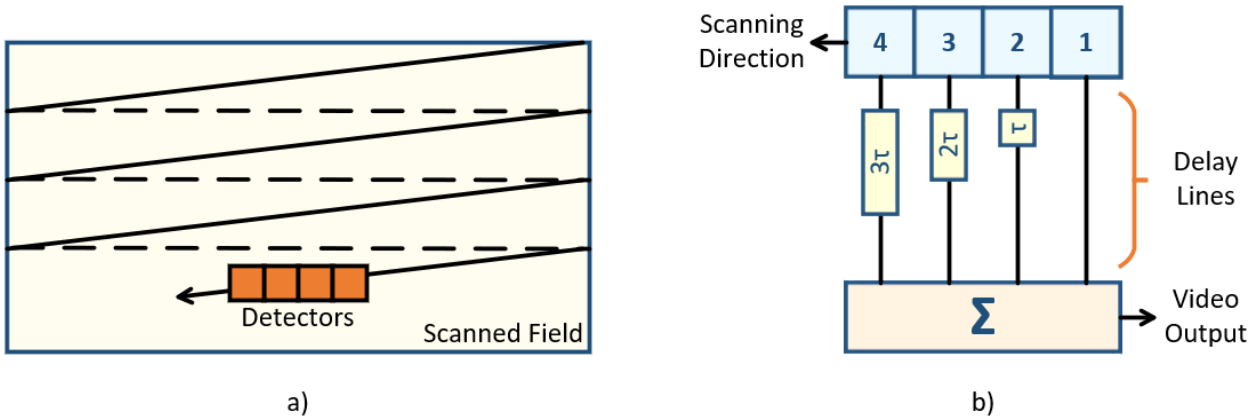

Figure 3. a) *The method of Staring FLIR,* ***b)*** *Delay Lines*

3. SYSTEM REQUIREMENTS RESULT ANALYSIS

System requirements can be grouped under three main categories. The first is related to image quality, the second is related to field performance, and the third is the category of requirements related to resource cost (size, weight, power requirement, etc.). Most of these requests require different engineering solutions to design an electro-optical thermal camera system. The design trade-off to meet the criteria determines the system's success. In this study, especially, evaluations related to field performance requirements will be included.

3.1. Field Performance Requirements

One of the most basic requirements for the user is to see sufficient detail at a certain distance. This requirement is provided by meeting objects' detection, diagnosis, and recognition functions. However, different levels of detail are required depending on the application area. For example, while it is sufficient for a security camera system to detect only human presence from a few hundred meters, it may be necessary to obtain an image in detail to be identified from a distance of 10 kilometers in a weapon system.

Spatial resolution is an essential parameter for the level of detail. However, since this parameter is related to the number of pixels of the detector, resolution/price is evaluated regarding availability (Biberman, 1975).

Considering the temperature differences, atmospheric permeability, and noise on the surfaces of the objects to be imaged, it is seen that the image contrast is as important a parameter as the resolution. The parameter used to measure the image contrast is the MRT value. This value is measured by a 7-line pattern formed by four hot sticks with three equal spaces between them. This pattern is called an MRT-type target. The calculations for detecting the MRT target at ΔT temperature at a specific atmospheric transmittance at a distance R are examined below to evaluate the field performance.

3.2. Field Performance Calculations

When the atmospheric permeability is represented with the propagation constant β, the temperature to be perceived by the system, ΔT_A, can be found by the following equation.

$$\Delta T_A = \Delta T e^{-\beta R} \qquad [K] \tag{6}$$

On an MRT-type target, a line (1/7th of the total pattern) is angularly denoted by ΔΦ.

$$\Delta\Phi = \frac{S}{7.R} \qquad [mrad] \tag{7}$$

where S indicates the total width of the 7-line MRT target (m), and R refers to the distance of the target (km).

Using (7), the target frequency can be determined as follows.

$$f = \frac{1}{2\Delta\Phi} = \left(\frac{3.5}{S}\right) R \; [cycles.mrad^{-1}] \tag{8}$$

R_0 is given as

$$R_0 = \frac{S}{7.\Delta\theta}\,[km] \tag{9}$$

The following equation (10) gives the system reference frequency f_0.

$$\frac{f}{f_0} = \frac{\Delta\theta}{\Delta\Phi} = \frac{R}{R_0} \tag{10}$$

(11) is valid since the temperature required to detect the target with sufficient resolution is MRT at the target frequency.

$$\Delta T.e^{-\beta R} = MRT\left(\frac{R}{R_0}\right)[K] \tag{11}$$

(11) is the fundamental equation for determining the sensing distance of a system. Both sides of the equation are plotted as a function of range, R, and propagation constant, β, and the intersection point gives the range at which detection can be made (Figure 4).

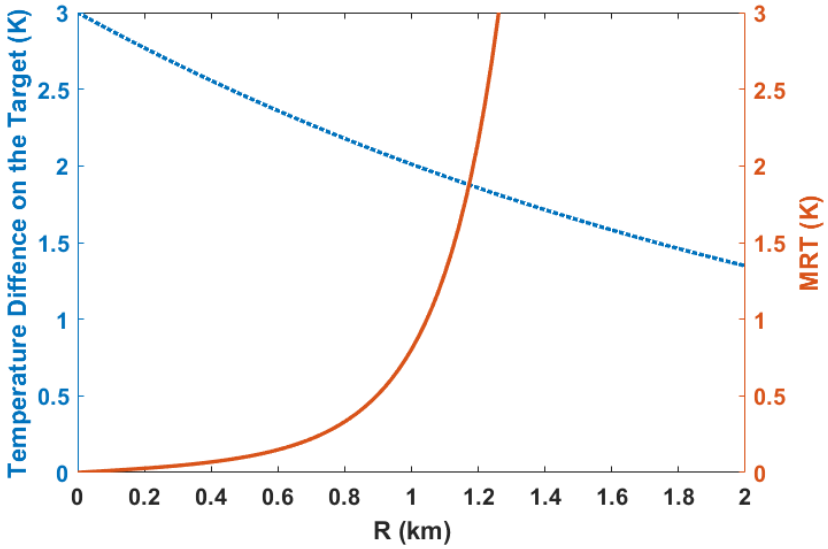

Figure 4. *The Aperture of the System is A_R=0.7, the System Output Noise Equivalent Temperature is NET*=0.14°C, and the Atmospheric Reduction Coefficient is β=0.4km^{-1}*

However, range calculations using (11) can be useful for systems with specified parameters. To be able to analyze, it is necessary to use functions that depend on parameters. By this way, it is possible to investigate what parameter impacts the range in which way. The starting point for this is the following equation.

$$MRT\left(\frac{R}{R_0}\right) \cong 0.7NET^*\left(\frac{R}{R_0}\right)exp\left[\alpha\left(\frac{R}{R_0}\right)^2\right] \tag{12}$$

To combine equations (11) and (12), we can define:

$$\alpha = -\ln MTF_S(1) \quad and \quad \gamma = \frac{\Delta T}{0.7NET^*} \tag{13}$$

So, (11) and (12) can be written as:

$$\ln\gamma - \beta R = \ln\left(\frac{R}{R_0}\right) + \alpha\left(\frac{R}{R_0}\right)^2 \tag{14}$$

R/R_0 logarithm can be expanded approximately as follows:

$$\ln\left(\frac{R}{R_0}\right) \cong \left(\frac{R}{R_0 - 1}\right) - \frac{1}{2}\left(\frac{R}{R_0 - 1}\right)^2 \tag{15}$$

When equation (15) is substituted into (14):

$$\left(\alpha - \frac{1}{2}\right)\left(\frac{R}{R_0}\right)^2 + 2\left(\frac{R}{R_0}\right) - \left(\frac{3}{2} + \ln\gamma - \beta R\right) = 0 \tag{16}$$

Then, R/R_0 can be found as:

$$\frac{R}{R_0} = \frac{\left[1 + \left(\alpha - \frac{1}{2}\right)\left(\frac{3}{2} + \ln\gamma - \beta R\right)\right]^{\frac{1}{2}}}{\left(\alpha - \frac{1}{2}\right)} \tag{17}$$

The relation between the system relative aperture A_R and the aperture D_0 of the optical part is defined as

$$A_R = D_0 \Delta\theta \tag{18}$$

The equation between R_0 and D_0 is given in (19).

$$R_0 = \frac{S}{7\Delta\theta} = \left(\frac{S}{7A_R}\right) D_0 \tag{19}$$

Substituting equation (19) in (17), the following formula for the optical aperture is obtained.

$$D_0 = \left\{ \frac{7\left(\alpha - \frac{1}{2}\right)\left(\frac{A_R}{S}\right)}{\left[1 + \left(\alpha - \frac{1}{2}\right)\left(\frac{3}{2} + ln\,\gamma - \beta R\right)\right]^{\frac{1}{2}} - 1} \right\} R \tag{20}$$

When the target's temperature, height, atmospheric transmittance coefficient, and system parameters are known as A_R, NET*, and MTF_S, the optical aperture value should be used to detect the target from a certain distance can be obtained by using (20). The system parameters A_R, NET*, and MTF_S depend on each other.

$$NET^* = \left(\eta_S^{1/2} A_R\right)^{-1} NET_0 \tag{21}$$

where η_S is the efficiency of the FLIR system (proportional to the square root of the number of detector pixels in the system).

$$MTF_S(1) = 0.64\left(\frac{4A_R - 1}{4A_R}\right) MTF_D(1) \tag{22}$$

(20), (21), and (22) are sufficient for many analyses.

3.3. Field Performance Sample Calculation

In this chapter, the calculations for a linear detector array with 120 elements positioned vertically and scanning horizontally are given. The index is used as "2:1 interlace" to output in 240x380 format. The values used in the calculations are given in Table 1. The system parameters obtained using the values in Table 1 are given in Table 2.

Table 1. *Optic and Detector Parameters*

Parameters	**Symbol**	**Value**
IR optic aperture	D_0	*4 in*
IR optic focal length	f_l	*11.4 in*
IR transmission	τ_o	*0.70*
IR optic design haze	σ_o	*0.058mrad*
Scanning efficiency	ε_s	*0.70*
Cold-shield efficiency	η_{cs}	*0.42*
Detector elements	N	*120*
Detector element size	$\omega_x\ \omega_x$	*2.0x2.0mils*^{2}
Detector efficiency	η_D	*0.10*
Spectral range	λ_1, λ_2	*8.0-10.0μm*

Table 2. *The System Parameters Calculated Using the Values in Table 1*

Parameters	**Equations**	**Values**
Δθ	ω / f_l	*0.175 (mrad)*
f_o	$1/2\ \Delta\theta$	*2.86 (cycles.mrad^{-1})*
$(FOV)_y$	$240\ \Delta\theta$	*42.0 (mrad)*
$(FOV)_x$	$320\ \Delta\theta$	*56.0 (mrad)*
A_R	$D_o\ \Delta\theta$	*0.70*
η_{cov}	$N\ \Delta\theta^2/(FOV)_x(FOV)_y$	*1.56x10^{-3}*
η_s	$\tau_o\varepsilon_s^{1/2}\ \eta_{cov}^{1/2}\eta_{cs}^{1/2}\ \eta_D^{1/2}$	*4.76x10^{-3}*
NET_0	$\left(\frac{7.87{M_q}^{1/2}}{M_q'{\tau_F}^{1/2}}\right)$	*4.58x10^{-4} (ºC)*
G_0	$(\eta_s D_o)^{-2} NET_0^2$	*5.79x10^{-5} (ºC^{2}mrad^2)*
*NET**	$G_0^{1/2}\ \Delta\theta$	*0.14 (ºC)*

$$MTF_{diff}\left(\frac{f}{f_0}\right) = 1 - \left(\frac{1}{4A_R}\right)\left(\frac{f}{f_0}\right) = 1 - 0.36\left(\frac{f}{f_0}\right) \quad (23)$$

$$MTF_{det}\left(\frac{f}{f_0}\right) = \exp[-\pi(f_\infty)^2] = \exp\left[-0.086\left(\frac{f}{f_0}\right)^2\right] \quad (24)$$

$$MTF_{det}\left(\frac{f}{f_0}\right) = \text{sinc}\left[(\pi/2)\left(\frac{f}{f_0}\right)\right] \quad (25)$$

The multiplication of (23), (24), and (25) equations are shown as the "IR detector" in Figure 5.

The electronic display part can be considered a Gaussian curve with a value of 0.90 at f_0.

$$MTF_{\frac{elektronik}{display}}\left(\frac{f}{f_0}\right) = exp\left[-0.10\left(\frac{f}{f_0}\right)^2\right] \quad (26)$$

The modulus of the optical transfer function (contrast) vs. f/f_0 is depicted as an MTF curve in Figure 5. (resolution) using (26). MTF of the detector is 0.51 at 0.8 f/f_0. However, since it is 0.94 for the electronic display/signal processing unit, by multiplying those, the total system MTF is achieved to be 0.48 at 0.8 f/f_0.

The MRT value can also be found with the following equation.

$$MRT = 0.7\left(\frac{f}{f_0}\right)\left[\frac{NET^*}{MTF_S(f/f_0)}\right] = 0.098\left[\frac{f/f_0}{MTF_S(f/f_0)}\right] \quad (27)$$

The relationship between the MRT and f/f_0 for a typical FLIR system is seen in Figure 6 by using (27). The maximum range for classification or recognition is the range where the target/background ΔT matches MRT at the spatial frequency specified by the relevant criterion, as MRT is a function of spatial frequency.

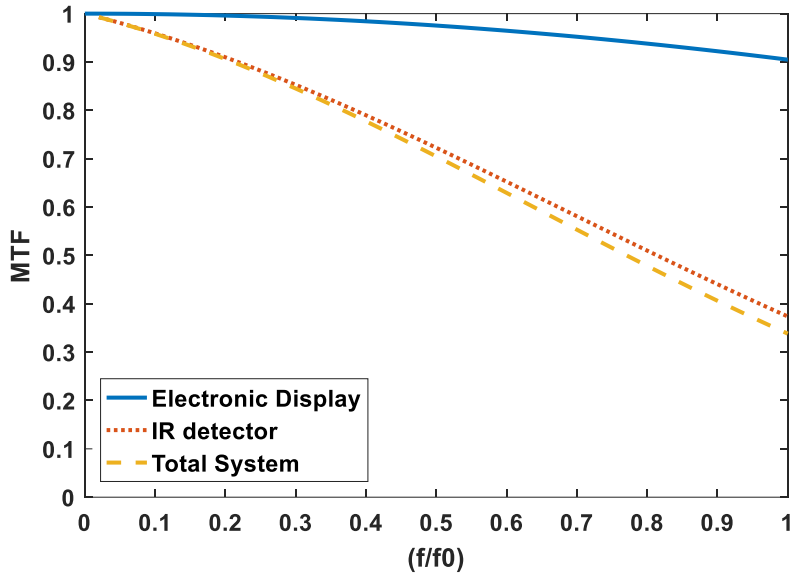

Figure 5. *MTF Analysis for the Designed Thermal Camera System*

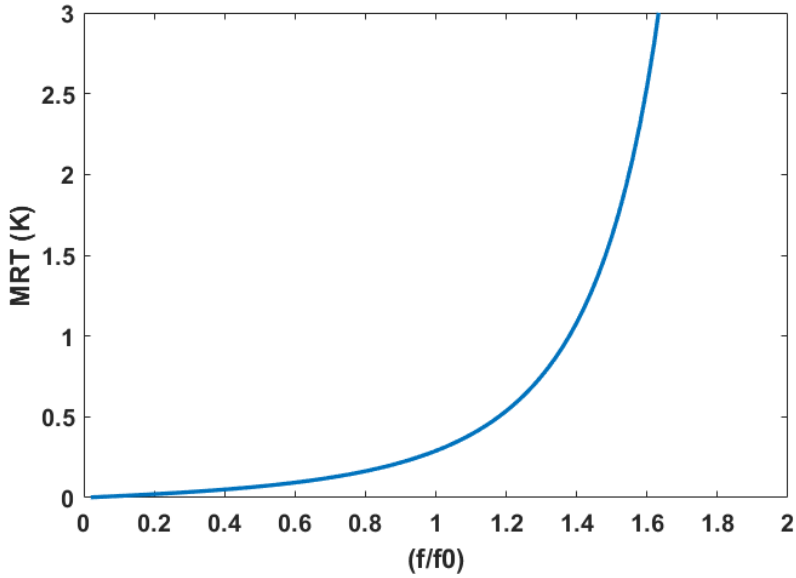

Figure 6. *MRT Analysis for the Designed Thermal Camera System*

Using the equations and Figure 6, the range at which an object with a width of 2 m and a temperature of 3ºC above the ambient temperature can be detected is calculated where the atmospheric permeability is 0.4 km^{-1}.

$$\alpha = -\ln MTF_S(1) = -\ln 0.339 = 1.0 \quad (28)$$

$$\gamma = \frac{\Delta T}{0.7NET*} = \frac{3}{0.098} = 30.6 \quad (29)$$

The values obtained by (28) and (29) are substituted in equation (20) and solved for R, the range is found to be 2.4 km.

$$R \cong 2.4km \quad (30)$$

4. CONCLUSION

Based on MRT characteristics, Johnson criteria enable the determination of the thermal camera range parameters. Since all the information pertinent to the scenario is unknown, it is difficult and sometimes impossible to provide simple answers regarding the range of a thermal imaging device. The solutions can be highly inaccurate even if all the data are known. Despite all the drawbacks, Johnson's criteria still apply for estimating the range of an IR thermal imager. Although IR thermal imaging system model improvements offer beneficial tools for analysis and synthesis that may be used during development for design optimization, imager range estimates in real-world settings are not significantly improved. Based on Johnson's criterion, IR thermal imaging systems produce MRT measurements, measurement results that also serve as a quality control tool to assess how well the image is made, and data that can be used to calculate the predefined target and distance of the imager. In this study, we calculated the field range performance of the system by defining the optical and detector parameters to obtain the fundamental parameters of the thermal camera system that we designed briefly. The range value (R) obtained from these calculations confirmed that range performance could also vary significantly in a thermal imaging system design depending on target dimensions, ambient temperature, and atmospheric transmittance.

CONFLICT OF INTEREST

The author declares no conflict of interest.

REFERENCES

Biberman, L. M. (1975). Displays and Perception of Displayed Information Seminar Series, University of Tel Aviv, 1–10 September 1974. *Applied Optics*, *14*(4), 800. doi:10.1364/ao.14.000800

Driggers, R. G., Vollmerhausen, R. H., & Krapels, K. A. (2000). Target identification performance as a function of low spatial frequency image content. *Optical Engineering*, *39*(9), 2458-2462. doi:10.1117/1.1288362

Hou, F., Zhang, Y., Zhou, Y., Zhang, M., Lv, B., & Wu, J. (2022). Review on infrared imaging technology. *Sustainability*, *14*(18), 11161. doi:10.3390/su141811161

Javidi, B. (Ed.) (2006). *Optical Imaging Sensors and Systems for Homeland Security Applications*. New York: Springer. doi:10.1007/b137387

Johnson, J. (1958, October 6-7). *Analysis of imaging forming systems*. In: Proceedings of the Image Intensifier Symposium (pp. 249-273). Ford Belvoir, VA.

Krapels, K., Driggers, R. G., Larson, P., Garcia, J., Walden, B., Agheera, S., Deaver, D., Hixson, J., & Boettcher, E. (2008, March 16-20). *Small craft ID criteria (N_{50}/V_{50}) for short wave infrared sensors in maritime security*. In: G. C. Holst (Eds.), Proceedings of the Infrared Imaging Systems: Design, Analysis, Modeling, and Testing XIX, 694108, Orlando, Florida, United States. SPIE. doi:10.1117/12.778062

Krapels, K., Deaver, D., & Driggers, R. (2006, September 11-14). *Small craft identification discrimination criteria N_{50} and V_{50} for visible and infrared sensors in maritime security*. In: R. G. Driggers & D. A. Huckridge (Eds.), Proceedings of the Electro-Optical and Infrared Systems: Technology and Applications III, 63950T, Stockholm, Sweden. SPIE. doi:10.1117/12.689140

Moyer, S. K., Hixson, J. G., Edwards, T. C., & Krapels, K. A. (2006). Probability of identification of small hand-held objects for electro-optic forward-looking infrared systems. *Optical Engineering*, *45*(6), 063201. doi:10.1117/1.2213997

Moyer, S. K., Flug, E., Edwards, T. C., Krapels, K. A., & Scarbrough, J. (2004, April 12-16). *Identification of handheld objects for electro-optic/FLIR applications*. In: G. C. Holst (Eds.), Proceedings of the Infrared Imaging Systems: Design, Analysis, Modeling, and Testing XV, Orlando, Florida, United States. SPIE. doi:10.1117/12.542066

NATO Standardization Agency. (1995). Measurement of the Minimum Resolvable Temperature Difference (MRTD) of Thermal Cameras (NATO STANAG 4349).

NATO Research and Technology Organisation. (2003). Experimental Assessment Parameters and Procedures for Characterization of Advanced Thermal Imagers. No: RTO-TR-075(II). (Accessed: 01/03/2023) PDF

Perić, D., & Livada, B. (2019, June 3-6). *MRTD Measurements Role in Thermal Imager Quality Assessment*. In: S. Vukosavić, & B. Lončar (Eds.), Proceedings of 6th International Conference on Electrical, Electronic and Computing Engineering ((Ic)ETRAN 2019) in conjunction with 63rd National Conference on Electrical, Electronic and Computing Engineering (ETRAN), (pp. 336-340), Silver Lake, Serbia.

Perić, D., Livada, B., Perić, M., & Vujić, S. (2019). Thermal imager range: Predictions, expectations, and reality. *Sensors*, *19*(15), 3313. doi:10.3390/s19153313

Sagan, V., Maimaitijiang, M., Sidike, P., Eblimit, K., Peterson, K. T., Hartling, S., Esposito, F., Khanal, K., Newcomb, M., Pauli, D., Ward, R., Fritschi, F., Shakoor, N., & Mockler, T. (2019). UAV-based high resolution thermal imaging for vegetation monitoring, and plant phenotyping using ICI 8640 P, FLIR Vue Pro R 640, and thermoMap cameras. *Remote Sensing*, *11*(3), 330. doi:10.3390/rs11030330

Schmieder, D. E., & Weathersby, M. R. (1983). Detection performance in clutter with variable resolution. *IEEE Transactions on Aerospace and Electronic Systems*, *AES-19*(4), 622-630. doi:10.1109/taes.1983.309351

Teaney, B. P., Reynolds, J. P., & O'Connor, J. (2007, April 9-13). *Guidance on methods and parameters for Army target acquisition models*. In: G. C. Holst (Eds.), Proceedings of the Infrared Imaging Systems: Design, Analysis, Modeling, and Testing XVIII, 65430L, Orlando, Florida, United States. SPIE. doi:10.1117/12.734511

U.S Army Night Vision and Electronic Sensors Directorate. (2001). Night Vision Thermal Imaging Systems Performance Model: User's Manual & Reference Guide. Fort Belvoir, VA.

Vollmer, M. (2021). Infrared Thermal Imaging. In: K. Ikeuchi (Eds.), *Computer Vision*, (pp. 666-670). Springer International Publishing. doi:10.1007/978-3-030-63416-2_844

Vollmerhausen, R. H., & Driggers, R. G. (2000). *Analysis of Sampled Imaging Systems*. SPIE Press, Bellingham, Washington USA. doi:10.1117/3.353257

Vollmerhausen, R. H., Reago Jr., D. A., & Driggers, R. G. (2010). *Analysis and Evaluation of Sampled Imaging Systems*. SPIE Press, Bellingham, Washington USA. doi:10.1117/3.853462

Vollmerhausen, R. H., & Jacobs, E. (2004). The Targeting Task Performance (TTP) Metric A New Model for Predicting Target Acquisition Performance. Defense Technical Information Center Technical Report, No: ADA422493.

Wolfe, W. L., & Zissis, G. J. (1985). *The Infrared Handbook*, Revised Edition. SPIE Press.